

## 3-D Shape Recovery from Image Brightness for non-Lambertian Surface

Wen Biao Jiang, Hai Yuan Wu and Tadayoshi Shioyama

Department of Mechanical and System Engineering, Kyoto Institute of Technology, Matsugasaki, Sakyo-ku, Kyoto 606, Japan, E-mail: shioyama@ipc.kit.ac.jp

This report presents a method for recovery of shape from shading in the case of a non-Lambertian surface illuminated by only a single light source. In the method, we derive simultaneous equations that should be satisfied by parameters determining reflectance map. After identifying the parameters by solving these equations, the surface normal is estimated by the iterative method using the surface normal information on the occluding boundary, and 3-D shape is recovered. The experimental results show the effectiveness of our method for shape from shading.

Journal of Imaging Science and Technology 41: 429–437 (1997)

### Introduction

The brightness of an object within an image contains the information concerning the direction of incident ray, the surface normal of the object, and the viewing direction as suggested by Horn.<sup>1</sup> When the object surface is made of a material that acts as a Lambertian reflector, the brightness varies as the cosine of the angle between the incident ray and the surface normal. A Lambertian surface is a diffuse reflector with the property that a particular surface patch looks equally bright from all viewing directions and its brightness is proportional to the illumination falling on it. For the Lambertian case, classical shape-from-shading methods have been developed for the single image by Ikeuchi and Horn<sup>2</sup> and for two images by Onn and Bruckstein.<sup>3</sup>

In the real world, object surfaces are almost non-Lambertian. In non-Lambertian surface cases, it is difficult to recover 3-D shape from image brightness because the reflectance map varies depending on the type of surface material of the object. For shape recovery in non-Lambertian case, photometric stereo methods have been developed by many researchers.<sup>4–8</sup> The previous photometric stereo procedures use multiple images of an object taken under different illumination conditions to estimate parameters determining the reflectance map and the surface normal. Because the previous methods are based on multiple images of an object sequentially illuminated by multiple light sources, they are considered impossible to be applied to natural scene understanding. Furthermore, when the observed object is moving, the previous methods give rise to a correspondence problem of points among multiple images because of sequential illumination.

For the purpose of natural scene understanding such as by the human retina, in this report, we propose a method

for shape recovery from image brightness of an object with a non-Lambertian surface illuminated by only a single light source. In the method, from the single image, we derive simultaneous equations that should be satisfied by the parameters determining the reflectance map. After obtaining the parameters by solving these equations, the normal of the object surfaces are estimated by an iterative algorithm, and 3-D shape is recovered. We theoretically consider the convergence of the proposed iterative algorithm. Furthermore, to evaluate the algorithm, experimental results are shown.

### Algorithm for 3-D Shape Inference

We assume orthographic image projection and let the viewing direction  $\mathbf{r}$  be parallel to the  $z$  axis. Then, the 3-D shape of an object can be described by its height,  $z$ , at coordinate  $(x, y)$  in the image plane. We denote by  $\mathbf{n}$  a unit vector normal to the surface of the object and by  $\mathbf{i}$  a unit vector in the direction of the light source. We assume parallel incident light. The vectors  $\mathbf{n}$  and  $\mathbf{i}$  are described by points on the unit sphere called the Gaussian sphere. In the stereographic projection, a point on the Gaussian sphere is projected by a ray through the point from the south pole onto the tangent plane at the north pole, which is called the stereographic plane. The coordinates  $(f, g)$  in the stereographic plane are given as follows:

$$f = 2p \left[ \sqrt{1 + p^2 + q^2} - 1 \right] / (p^2 + q^2), \quad (1)$$

$$g = 2q \left[ \sqrt{1 + p^2 + q^2} - 1 \right] / (p^2 + q^2), \quad (2)$$

where  $p$  and  $q$  are defined as

$$p \equiv \frac{\partial z}{\partial x}, \quad q \equiv \frac{\partial z}{\partial y}, \quad (3)$$

and are related to  $f$  and  $g$  as follows:

$$p = 4f / (4 - f^2 - g^2), \quad q = 4g / (4 - f^2 - g^2). \quad (4)$$

Original manuscript received November 10, 1996.

\* On leave from the Institute of Solid State Physics, Bulgarian Academy of Sciences, 72, Tzarigradsko Chaussee Blvd., 1784 Sofia, Bulgaria

The unit vector  $\mathbf{r}$  and the surface normal  $\mathbf{n}$  are given by

$$\mathbf{r} = (0, 0, 1), \quad \mathbf{n} = (-p, -q, 1) / \sqrt{1 + p^2 + q^2}, \quad (5)$$

The vectors  $\mathbf{n}$  and  $\mathbf{i}$  are described in terms of  $f$  and  $g$  as follows:

$$\mathbf{n} = [-4f, -4g, 4 - f^2 - g^2] / (4 + f^2 + g^2), \quad (6)$$

$$\mathbf{i} = [-4f_i, -4g_i, 4 - f_i^2 - g_i^2] / (4 + f_i^2 + g_i^2), \quad (7)$$

where  $(f_i, g_i)$  denote the stereographic coordinates corresponding to the direction of the light.

We assume that the viewing direction coincides with the north pole of the Gaussian sphere and that points on the northern hemisphere of the Gaussian sphere are considered. Therefore, the considered points  $(f, g)$  and  $(f_i, g_i)$  in the stereographic plane are constrained to the following regions:

$$f^2 + g^2 \leq 4, \quad f_i^2 + g_i^2 \leq 4.$$

When the object surface material exhibits non-Lambertian reflection, the reflectance map is given by<sup>6,9</sup>

$$R(\mathbf{i}, \mathbf{n}, \mathbf{r}) = \begin{cases} \rho_1 \exp\left\{-c^2 \left[\cos^{-1}(n_s \cdot \mathbf{n})\right]^2\right\} + \rho_2 (\mathbf{i} \cdot \mathbf{n}), & \text{if } (\mathbf{i} \cdot \mathbf{n}) > 0, \\ 0, & \text{otherwise,} \end{cases} \quad (8)$$

where the symbol  $\cdot$  denotes a scalar product,

$$\mathbf{n}_s \equiv (\mathbf{i} + \mathbf{r}) / \|\mathbf{i} + \mathbf{r}\|$$

is the specular direction, and  $c$  is a constant that depends on the surface roughness. The value of  $c^2$  has information about non-Lambertian scatter near the specular direction. For the surface in this report the value of  $c$  is set<sup>6</sup> as 2.578,  $\rho_1$  is the specular reflectivity,  $\rho_2$  is the Lambertian component, and  $\rho_1$  and  $\rho_2$  are called the parameter determining reflectance property.

**Estimating  $\rho_1$  and  $\rho_2$ .** In this section, we use the zenith and azimuth angle  $\theta$  and  $\phi$  to represent unit vectors, and the convention we adopt with respect to these is as follows: The zenith angle of any unit vector is measured positively down from the  $z$  axis while the azimuth angle is measured positively counterclockwise from the  $x$  axis. The  $\theta$  and  $\phi$  usually are subscripted indicating to which vectors they belong. Thus,  $\theta_n$  and  $\phi_n$  are zenith and azimuth angles, respectively, of the vector  $\mathbf{n}$  while  $\theta_i$  and  $\phi_i$  are the angles of  $\mathbf{i}$ . Then we have the following relations:

$$\mathbf{n} = (\sin\theta_n \cos\phi_n, \sin\theta_n \sin\phi_n, \cos\theta_n), \quad (9)$$

$$\mathbf{i} = (\sin\theta_i \cos\phi_i, \sin\theta_i \sin\phi_i, \cos\theta_i), \quad (10)$$

$$(\mathbf{i} \cdot \mathbf{n}) = \mathbf{i}_x \mathbf{n}_x + \mathbf{i}_y \mathbf{n}_y + \mathbf{i}_z \mathbf{n}_z = \cos\theta_i \cos\theta_n + \sin\theta_i \sin\theta_n \cos(\phi_i - \phi_n). \quad (11)$$

Because viewing direction  $\mathbf{r}$  is along the  $z$  axis and  $\mathbf{n}_s$  lies in the principal plane spanned by  $\mathbf{i}$  and  $\mathbf{r}$ , the zenith and azimuth angle of  $\mathbf{n}_s$  are  $\theta_s = \theta_i/2$ ,  $\phi_s = \phi_i$ . Then  $(\mathbf{n}_s \cdot \mathbf{n})$  is given by

$$(\mathbf{n}_s \cdot \mathbf{n}) = \cos \frac{\theta_i}{2} \cos \theta_n + \sin \frac{\theta_i}{2} \sin \theta_n \cos(\phi_i - \phi_n). \quad (12)$$

When we denote by  $E$  the brightness normalized such that its maximum value is equal to 1, we obtain the image irradiance equation:

$$E = R(\mathbf{i}, \mathbf{n}, \mathbf{r}). \quad (13)$$

Because the mapping from unit vectors to zenith and azimuth angles is one to one, Eq. 13 can be written as follows:

$$E = R(\theta_n, \phi_n) = \rho_1 \exp\left\{-c^2 \left[\cos^{-1}\left(\cos \frac{\theta_i}{2} \cos \theta_n + \sin \frac{\theta_i}{2} \sin \theta_n \cos(\phi_i - \phi_n)\right)\right]^2\right\} + \rho_2 [\cos \theta_i \cos \theta_n + \sin \theta_i \sin \theta_n \cos(\phi_i - \phi_n)]. \quad (14)$$

It is considered that the right side of Eq. 14 takes maximum value  $R_{\max}$  at a vector in the principal plane, i.e.,  $\phi_n = \phi_i$ . Hence,  $R_{\max}$  is obtained by finding the maximum value of  $R(\theta_n, \phi_n = \phi_i)$ , i.e., by finding the solution  $\theta_n^*$  of

$$\frac{\partial}{\partial \theta_n} R(\theta_n, \phi_n = \phi_i) = 0.$$

Then  $\rho_1$  and  $\rho_2$  should satisfy

$$R_{\max} = R(\theta_n^*, \phi_n^*) = 1, \quad (15)$$

where we assume that  $(\theta_i, \phi_i)$  are known and  $\theta_i < \pi/2$ . For  $\phi_n = \phi_i$ ,  $R(\theta_n, \phi_n)$  is given by

$$R(\theta_n, \phi_i) = \rho_1 \exp\left\{-c^2 \left(\theta_n - \frac{\theta_i}{2}\right)^2\right\} + \rho_2 \cos(\theta_n - \theta_i). \quad (16)$$

The equation

$$\frac{\partial}{\partial \theta_n} R(\theta_n, \phi_n = \phi_i) = 0$$

leads to

$$\rho_1 2c^2 \left(\theta_n^* - \frac{\theta_i}{2}\right) \exp\left\{-c^2 \left(\theta_n^* - \frac{\theta_i}{2}\right)^2\right\} + \rho_2 \sin(\theta_n^* - \theta_i) = 0. \quad (17)$$

Hence,  $\rho_1$ ,  $\rho_2$  and  $\theta_n^*$  should satisfy the following simultaneous equations:

$$\rho_1 2c^2 \left(\theta_n^* - \frac{\theta_i}{2}\right) \exp\left\{-c^2 \left(\theta_n^* - \frac{\theta_i}{2}\right)^2\right\} + \rho_2 \sin(\theta_n^* - \theta_i) = 0, \quad (18)$$

$$\rho_1 \exp\left\{-c^2 \left(\theta_n^* - \frac{\theta_i}{2}\right)^2\right\} + \rho_2 \cos(\theta_n^* - \theta_i) = 1. \quad (19)$$

Here, we assume that the surface material is homogeneous and  $\rho_1$  and  $\rho_2$  are constant over the surface.

The surface normal at a point on the occluding boundary is given by the unit vector perpendicular to the tangent

line of the silhouette of the occluding boundary in the image plane. Let  $(\bar{\theta}_n, \bar{\phi}_n)$  be a direction of surface normal at a point on the occluding boundary and  $\bar{E} \equiv E(\bar{\theta}_n, \bar{\phi}_n)$  be its brightness. Then we have

$$\rho_1 \exp \left\{ -c^2 \left[ \cos^{-1} \left( \cos \frac{\theta_i}{2} \cos \bar{\theta}_n + \sin \frac{\theta_i}{2} \sin \bar{\theta}_n \cos(\phi_i - \bar{\phi}_n) \right) \right]^2 \right\} + \rho_2 \left[ \cos \theta_i \cos \bar{\theta}_n + \sin \theta_i \sin \bar{\theta}_n \cos(\phi_i - \bar{\phi}_n) \right] = \bar{E}. \quad (20)$$

Because we assume the property of reflection on the surface material is homogeneous, we can obtain  $\rho_1$ ,  $\rho_2$ , and  $\theta_n^*$  by solving the simultaneous Eqs. 18 through 20. In this report we use the Newton iterative algorithm to solve the simultaneous equations.

After obtaining  $\rho_1$ ,  $\rho_2$ , and  $\theta_n^*$  by the method mentioned above, we estimate surface normal using Eq. 13 and the property of occluding boundary.

**Surface Normal Inference.** In the sequel, at each considered point in the image plane, Eq.13 is rewritten as

$$E_{ij} = R(f_{ij}, g_{ij}), \quad (21)$$

where  $(f_{ij}, g_{ij})$  denote the stereographic coordinates corresponding to the surface normal at image plane coordinate  $(i, j)$ . We define the constraint  $h_1(f, g)$  as

$$h_1(\mathbf{u}) \equiv E - R(\mathbf{u}) = 0, \quad (22)$$

$$\mathbf{u} \equiv (u_1, u_2)^t \equiv (f_{ij}, g_{ij})^t, \quad (23)$$

which is imposed on the image brightness, where  $t$  denotes the transpose operator. We use the following Marquardt method<sup>10</sup> to estimate surface normal. The Marquardt method is a combination of the Newton method and the method of steepest descent.

At each considered point in the image, the estimate  $\mathbf{u}^{(v)}$  at the  $v$ -th iteration is improved with  $\Delta \mathbf{u}$  in the following steps.

1. Solve the following equation with unknown vector  $\Delta \mathbf{u} \equiv (\Delta u_1, \Delta u_2)^t \equiv (\Delta f_{ij}, \Delta g_{ij})^t$ ,

$$\left[ G_1(\mathbf{u}^{(v)}) + \lambda I \right] \Delta \mathbf{u} = - \frac{\partial W(\mathbf{u}^{(v)})}{\partial \mathbf{u}}, \quad (24)$$

where  $I$  denotes a  $2 \times 2$  dimensional identity matrix and  $W(\mathbf{u})$ ,  $G_1$ , and  $J_1$ , are defined as

$$W(\mathbf{u}) \equiv \frac{1}{2} h_1^2, \quad G_1 \equiv J_1^t J_1, \quad (25)$$

$$\frac{\partial W(\mathbf{u})}{\partial \mathbf{u}} = h_1 J_1, \quad J_1 \equiv \frac{\partial \mathbf{h}_1}{\partial \mathbf{u}} : \text{Jacobian}. \quad (26)$$

2. Improve the estimate  $\mathbf{u}^{(v)}$  as follows:

$$\mathbf{u}^{(v+1)} = \mathbf{u}^{(v)} + \Delta \mathbf{u}. \quad (27)$$

Solving Eq. 24,  $\Delta \mathbf{u}$  is given by

$$\Delta \mathbf{u}_1^{(v)} \equiv \Delta f_{i,j}^{(v)} = \frac{E_{i,j} - R(f_{i,j}^{(v)}, g_{i,j}^{(v)})}{R_f(f_{i,j}^{(v)}, g_{i,j}^{(v)})^2 + R_g(f_{i,j}^{(v)}, g_{i,j}^{(v)})^2 + \gamma} R_g(f_{i,j}^{(v)}, g_{i,j}^{(v)}), \quad (28)$$

$$\Delta \mathbf{u}_2^{(v)} \equiv \Delta g_{i,j}^{(v)} = \frac{E_{i,j} - R(f_{i,j}^{(v)}, g_{i,j}^{(v)})}{R_f(f_{i,j}^{(v)}, g_{i,j}^{(v)})^2 + R_g(f_{i,j}^{(v)}, g_{i,j}^{(v)})^2 + \gamma} R_f(f_{i,j}^{(v)}, g_{i,j}^{(v)}), \quad (29)$$

where

$$R_f \equiv \frac{\partial R}{\partial f}, \quad R_g \equiv \frac{\partial R}{\partial g}. \quad (30)$$

In the above algorithm, the value of  $\mathbf{u}$  at a point on the occluding boundary is known.<sup>2</sup> The initial value of  $\mathbf{u}$  at a point on the region except the occluding boundary, is set as  $\mathbf{u} = \mathbf{0}$ . For convenience, the region where  $\mathbf{u} = \mathbf{0}$  and  $\mathbf{u}$  is not yet improved, is called the unknown region. The estimate  $\mathbf{u}^{(v)}$  at a point on the unknown region can be obtained from the following two steps:

1. When there is at least one point called the known point, which does not belong to an unknown region, in the eight neighboring points, we have

$$f_{ij}^{(v)} = a \bar{f}_{ij}^{(v)} + b \hat{f}_{ij}^{(v)},$$

$$g_{ij}^{(v)} = a \bar{g}_{ij}^{(v)} + b \hat{g}_{ij}^{(v)},$$

where

$$\bar{f}_{ij} \equiv f_{i+1,j} + f_{i,j+1} + f_{i-1,j} + f_{i,j-1},$$

$$\bar{g}_{ij} \equiv g_{i+1,j} + g_{i,j+1} + g_{i-1,j} + g_{i,j-1},$$

$$\hat{f}_{ij} \equiv f_{i-1,j-1} + f_{i+1,j-1} + f_{i-1,j+1} + f_{i+1,j+1},$$

$$\hat{g}_{ij} \equiv g_{i-1,j-1} + g_{i+1,j-1} + g_{i-1,j+1} + g_{i+1,j+1}.$$

If in the four immediate neighbors  $(i \pm 1, j)$ ,  $(i, j \pm 1)$ , there exists a known point,  $(a, b) = (1/c_1, 0)$ , and  $c_1$  is the number of known points in the four immediate neighbors, else  $(a, b) = (0, 1/c_2)$  and  $c_2$  is the number of known points in the eight neighboring points.

2. In the case other than Step 1,

$$f_{ij}^{(v)} = g_{ij}^{(v)} = 0.$$

Because the unknown region will vanish as the iteration goes ahead, the above two steps are used only as transient process.

After obtaining  $(f, g)$  by the above algorithm, we can have  $(p, q)$  by Eq. 4 and from Eq. 3 we can obtain the height  $z$  by integrating  $p$  and  $q$ . Thus, we can reconstruct the 3-D shape.

### Convergence of Iterative Algorithm

In this section, we theoretically consider convergence of the iterative algorithm. We define  $\mathbf{X}$ ,  $\mathbf{h}(\mathbf{X})$ ,  $W(\mathbf{X})$  and  $G(\mathbf{X})$  as

$$\mathbf{X} \equiv \left[ (f_{ij}, g_{ij}), (i, j) \in \Omega \right]^t \equiv \left[ \mathbf{X}_{ij1}, \mathbf{X}_{ij2}, (i, j) \in \Omega \right]^t, \quad (31)$$

$$\mathbf{h}(\mathbf{X}) \equiv \left[ (E_{ij} - R(f_{ij}, g_{ij})), (i, j) \in \Omega \right]^t \equiv [h_{ij}, (i, j) \in \Omega]^t, \quad (32)$$

$$W(\mathbf{X}) \equiv \frac{1}{2} \mathbf{h}(\mathbf{X})^t \mathbf{h}(\mathbf{X}), \quad (33)$$

$$G(\mathbf{X}) \equiv J^t J, \quad J \equiv \frac{\partial \mathbf{h}(\mathbf{X})}{\partial \mathbf{X}}: \text{Jacobian}, \quad (34)$$

where  $\Omega$  is defined as the set of orthographic image projections of points on the observed surface of the object. Then, we have

$$\frac{\partial W(\mathbf{X})}{\partial \mathbf{X}} = \mathbf{h}(\mathbf{X})^t J. \quad (35)$$

The Marquardt algorithm in section “**Estimating  $\rho_1$  and  $\rho_2$** ” is rewritten as

$$\mathbf{X}^{(v+1)} = Y\mathbf{X}^{(v)}, \quad (36)$$

$$Y\mathbf{X} \equiv \mathbf{X} + B(\mathbf{X})^{-1}F(\mathbf{X}), \quad (37)$$

$$B(\mathbf{X})^{-1} \equiv [G(\mathbf{X}) + \gamma I]^{-1}, \quad (38)$$

$$F(\mathbf{X}) \equiv -\frac{\partial W(\mathbf{X})}{\partial \mathbf{X}}, \quad (39)$$

where  $\mathbf{X}^{(v)}$  is the value at the  $v$ -th iteration. At the true solution  $\mathbf{X}^*$ , we have  $F$ -derivative of  $Y$ :

$$Y'(\mathbf{X}^*) = I + B(\mathbf{X}^*)^{-1}F'(\mathbf{X}^*), \quad (40)$$

where  $I$  denotes the identity matrix.

Next, let us consider the spectral radius  $\rho [Y'(\mathbf{X}^*)]$  of  $Y'(\mathbf{X}^*)$ . Expanding  $W(\mathbf{X})$  around  $\mathbf{X}^*$  by the Taylor expansion, we have

$$W(\mathbf{X}) = \frac{1}{2} \left\{ \mathbf{h}(\mathbf{X}^*) + J(\mathbf{X} - \mathbf{X}^*) + O[(\mathbf{X} - \mathbf{X}^*)^2] \right\}^t \times \left\{ \mathbf{h}(\mathbf{X}^*) + J(\mathbf{X} - \mathbf{X}^*) + O[(\mathbf{X} - \mathbf{X}^*)^2] \right\}. \quad (41)$$

Because  $\mathbf{X} - \mathbf{X}^*$  is quite small, we neglect second-order terms. Then  $W(\mathbf{X})$  is approximated as

$$W(\mathbf{X}) \approx \frac{1}{2} (\mathbf{X} - \mathbf{X}^*)^t J^t J (\mathbf{X} - \mathbf{X}^*). \quad (42)$$

From Eq. 42, we can obtain

$$F'(\mathbf{X}) = -\frac{\partial^2 W}{\partial \mathbf{X}^2} = -J^t J = -G(\mathbf{X}), \quad (43)$$

$$Y'(\mathbf{X}) = I + [G(\mathbf{X}^*) + \gamma I]^{-1} [-G(\mathbf{X}^*) - \gamma I + \gamma I] = \gamma [G(\mathbf{X}^*) + \gamma I]^{-1}. \quad (44)$$

From Eq. 32, we can obtain

$$J_{ij,i'j'l} = \frac{\partial [\mathbf{h}(\mathbf{X})]_{ij}}{\partial \mathbf{X}_{i'j'l}} = -\delta_{ij,i'j'} R_l(f_{ij}, g_{ij}), \quad (45)$$

where

$$\delta_{ij,i'j'} \equiv \begin{cases} 1 & (\text{if } i' = i, j' = j), \\ 0 & (\text{otherwise}), \end{cases} \quad (46)$$

$$R_l(f_{ij}, g_{ij}) = \begin{cases} \frac{\partial R(f_{ij}, g_{ij})}{\partial f_{ij}} = \frac{\partial R(f_{ij}, g_{ij})}{\partial \mathbf{X}_{ij1}} & (l = 1), \\ \frac{\partial R(f_{ij}, g_{ij})}{\partial g_{ij}} = \frac{\partial R(f_{ij}, g_{ij})}{\partial \mathbf{X}_{ij2}} & (l = 2). \end{cases} \quad (47)$$

From Eqs. 34 and 45, the following can be obtained

$$G_{ijl,i'j'l} = \sum_{\bar{ij}} J_{ijl,\bar{ij}}^t J_{\bar{ij},i'j'l} = \quad (48)$$

$$J_{ijl,\bar{ij}}^t J_{\bar{ij},i'j'l} = \delta_{ij,i'j'} R_l R_l,$$

$$[G + \gamma I]_{ijl,i'j'l} = \delta_{ij,i'j'} \delta_{l,l} \gamma + \delta_{ij,i'j'} R_l(f_{ij}, g_{ij}) R_l(f_{ij}, g_{ij}), \quad (49)$$

$$[G + \gamma I] = \text{block-diag} [\tilde{D}_{ij}, (i, j) \in \Omega], \quad (50)$$

$$[G + \gamma I]^{-1} = \text{block-diag} [\tilde{D}_{ij}^{-1}, (i, j) \in \Omega], \quad (51)$$

where

$$\tilde{D}_{ij} \equiv \begin{bmatrix} \gamma + R_1(f_{ij}, g_{ij})^2 & R_1(f_{ij}, g_{ij}) R_2(f_{ij}, g_{ij}) \\ R_2(f_{ij}, g_{ij}) R_1(f_{ij}, g_{ij}) & \gamma + R_2(f_{ij}, g_{ij})^2 \end{bmatrix}, \quad (52)$$

$$\tilde{D}_{ij}^{-1} \equiv \frac{-1}{|\tilde{D}_{ij}|} \begin{bmatrix} -\gamma - R_2(f_{ij}, g_{ij})^2 & R_1(f_{ij}, g_{ij}) R_2(f_{ij}, g_{ij}) \\ R_2(f_{ij}, g_{ij}) R_1(f_{ij}, g_{ij}) & -\gamma - R_1(f_{ij}, g_{ij})^2 \end{bmatrix}, \quad (53)$$

and

$$|\tilde{D}_{ij}| = \gamma^2 + \gamma R_1(f_{ij}, g_{ij})^2 + \gamma R_2(f_{ij}, g_{ij})^2. \quad (54)$$

From Eq. 44, we have

$$Y'(\mathbf{X}^*) = \text{block-diag} [D_{ij}, (i, j) \in \Omega], \quad (55)$$

where

$$D_{ij} \equiv \frac{-\gamma}{|\tilde{D}_{ij}|} \begin{bmatrix} -\gamma - R_2(f_{ij}^*, g_{ij}^*)^2 & R_1(f_{ij}^*, g_{ij}^*) R_2(f_{ij}^*, g_{ij}^*) \\ R_2(f_{ij}^*, g_{ij}^*) R_1(f_{ij}^*, g_{ij}^*) & -\gamma - R_1(f_{ij}^*, g_{ij}^*)^2 \end{bmatrix}. \quad (56)$$

To determine the eigenvalue of  $Y'(\mathbf{X}^*) = \gamma [G + \gamma I]^{-1}$ , we first calculate the eigenvalue of  $[G + \gamma I]$ . Expanding the determinant  $|G + \gamma I - \mu I|$  by the Laplace expansion, we get

$$\begin{aligned}
|G + \gamma I - \mu I| &= \prod_{(i,j) \in \Omega} |\tilde{D}_{ij} - \mu I_2| \\
&= \prod_{(i,j) \in \Omega} \left| \begin{array}{cc} R_1(f_{ij}^*, g_{ij}^*)^2 + \gamma - \mu & R_1(f_{ij}^*, g_{ij}^*)R_2(f_{ij}^*, g_{ij}^*) \\ R_2(f_{ij}^*, g_{ij}^*)R_1(f_{ij}^*, g_{ij}^*) & R_2(f_{ij}^*, g_{ij}^*)^2 + \gamma - \mu \end{array} \right| \\
&= \prod_{(i,j) \in \Omega} [\mu^2 - (2\gamma + R_1^2 + R_2^2)\mu + \gamma(\gamma + R_1^2 + R_2^2)].
\end{aligned} \tag{57}$$

where  $I_2$  is  $2 \times 2$  unit matrix. The zero root of Eq. 57 is given by

$$\mu = \frac{(2\gamma + R_1^2 + R_2^2) \pm (R_1^2 + R_2^2)}{2}. \tag{58}$$

From Eqs. 44 and 58, we obtain the eigenvalue of  $Y(\mathbf{X}^*)$  as follows:

$$\mu_1 = \frac{\gamma}{(\gamma + R_1^2 + R_2^2)}, \quad \mu_2 = \frac{\gamma}{\gamma} = 1. \tag{59}$$

If the maximum eigenvalue is smaller than 1, the algorithm converges.<sup>10</sup> Because the eigenvalue  $\mu_2 = 1$ , it seems that the algorithm does not converge. However, we can verify the convergence of the algorithm by considering the improvement vector represented with the eigenvectors of eigenvalues  $\mu_1$  and  $\mu_2$  as follows:

For simplicity, we assume  $R_1 \neq 0$  or  $R_2 \neq 0$ . If  $R_1 = R_2 = 0$  is satisfied, then the value of  $R$  is maximum and the  $(f, g)$  can be obtained from solution  $\theta_n^*$  of simultaneous Eqs. 18 through 20 and  $\phi_n^* = \phi_i$ . So on inferring surface normal, we can assume  $R_1 \neq 0$  or  $R_2 \neq 0$  in the region other than the  $R_{\max}$  point. In the following, we solve the eigenvalue equation:

$$(\mu I - D_{ij})\mathbf{x} = 0, \tag{60}$$

where  $\mathbf{x} = (x_1, x_2)^t$ . When  $\mu = \mu_1$ , we have

$$R_2 x_1 - R_1 x_2 = 0. \tag{61}$$

Because  $R_1 \neq 0$  or  $R_2 \neq 0$ , vector  $\xi \equiv (\xi_1, \xi_2)^t \equiv (R_1, R_2)^t$  is a solution of Eq. 61 and vector  $\xi$  is an eigenvector corresponding to eigenvalue  $\mu_1$ . When  $\mu = \mu_2$ , Eq. 60 is described as

$$R_1 x_1 + R_2 x_2 = 0. \tag{62}$$

Vector  $\eta \equiv (\eta_1, \eta_2)^t \equiv (R_2, -R_1)^t$  is a solution of Eq. 62 and vector  $\eta$  is an eigenvector corresponding to eigenvalue  $\mu_2$ . Because

$$\begin{vmatrix} \xi_1 & \eta_1 \\ \xi_2 & \eta_2 \end{vmatrix} = \begin{vmatrix} R_1 & R_2 \\ R_2 & -R_1 \end{vmatrix} = -(R_1^2 + R_2^2) \neq 0, \tag{63}$$

vectors  $\xi, \eta$  are independent of each other. Then the improvement vector

$$\Delta \mathbf{X}_{ij}^{(v)} \equiv (\Delta \mathbf{X}_{ij1}^{(v)}, \Delta \mathbf{X}_{ij2}^{(v)})^t \equiv \mathbf{X}_{ij}^{(v+1)} - \mathbf{X}_{ij}^{(v)}$$

can be represented as a linear combination of  $\xi, \eta$ :

$$\Delta \mathbf{X}_{ij}^{(v)} = \alpha^{(v)} \xi + \beta^{(v)} \eta, \tag{64}$$

$$\begin{aligned}
\Delta \mathbf{X}_{ij}^{(v)} &= D_{ij} \Delta \mathbf{X}_{ij}^{(v-1)} = D_{ij} (\alpha^{(v-1)} \xi + \beta^{(v-1)} \eta), \\
&= \alpha^{(m)} \mu_1^{v-m} \xi + \beta^{(m)} \mu_2^{v-m} \eta
\end{aligned} \tag{65}$$

From Eqs. 28 and 29, for a sufficiently large  $m$ , we have

$$\begin{aligned}
\Delta \mathbf{X}_{ij}^{(m)} &= \begin{pmatrix} \Delta f_{ij}^{(m)} \\ \Delta g_{ij}^{(m)} \end{pmatrix} = \\
\alpha_{ij}^{(m)} &\begin{pmatrix} R_f(f_{ij}^{(m)}, g_{ij}^{(m)}) \\ R_g(f_{ij}^{(m)}, g_{ij}^{(m)}) \end{pmatrix} \approx \alpha_{ij}^{(m)} \begin{pmatrix} R_f(f_{ij}^*, g_{ij}^*) \\ R_g(f_{ij}^*, g_{ij}^*) \end{pmatrix} = \alpha_{ij}^{(m)} \xi.
\end{aligned} \tag{66}$$

where

$$\alpha_{ij}^{(m)} = \frac{E_{ij} - R(f_{ij}^{(m)}, g_{ij}^{(m)})}{R_f(f_{ij}^{(m)}, g_{ij}^{(m)})^2 + R_g(f_{ij}^{(m)}, g_{ij}^{(m)})^2 + \gamma}. \tag{67}$$

From Eqs. 65 and 66, we obtain  $\beta^{(v)} \approx 0$ . Therefore,  $\Delta \mathbf{X}_{ij}^{(v)}$  can be approximately represented as

$$\Delta \mathbf{X}_{ij}^{(v)} = D_{ij}^{v-m} \Delta \mathbf{X}_{ij}^{(m)} \approx D_{ij}^{v-m} \alpha_{ij}^{(m)} \xi = \alpha_{ij}^{(m)} \mu_1^{v-m} \xi, \tag{68}$$

where  $m$  is a sufficiently large number such that Eq. 66 holds. Equation 68 implies that the improvement of the estimate depends only on the eigenvalue of  $|\mu| < 1$ . Therefore, the algorithm converges.

**Dependence of Eigenvalue on  $\rho_i$ .** From Eqs. 4 and 5 and the unit vector  $\mathbf{r}$ , we have the following relations:

$$\mathbf{i} + \mathbf{r} = [-4f_i, -4g_i, 8] / (4 + f_i^2 + g_i^2), \tag{69}$$

$$\mathbf{n}_s = (\mathbf{i} + \mathbf{r}) / \|\mathbf{i} + \mathbf{r}\| = [-f_i, -g_i, 2] / \sqrt{4 + f_i^2 + g_i^2}, \tag{70}$$

$$(\mathbf{i} \cdot \mathbf{n}) = \frac{16(ff_i + gg_i) + (4 - f^2 - g^2)(4 - f_i^2 - g_i^2)}{(4 + f^2 + g^2)(4 + f_i^2 + g_i^2)}, \tag{71}$$

$$(\mathbf{n}_s \cdot \mathbf{n}) = \frac{4(ff_i + gg_i) + 2(4 - f^2 - g^2)}{(4 + f^2 + g^2)\sqrt{4 + f_i^2 + g_i^2}}, \tag{72}$$

$$\begin{aligned}
\frac{\partial}{\partial f} (\mathbf{i} \cdot \mathbf{n}) &= \\
&= \frac{8f_i - (4 - f^2 - g^2)f - (4 + f_i^2 + g_i^2)f(\mathbf{i} \cdot \mathbf{n})}{2(4 + f^2 + g^2)(4 + f_i^2 + g_i^2)},
\end{aligned} \tag{73}$$

$$\begin{aligned}
\frac{\partial}{\partial g} (\mathbf{i} \cdot \mathbf{n}) &= \\
&= \frac{8g_i - (4 - f^2 - g^2)g - (4 + f_i^2 + g_i^2)g(\mathbf{i} \cdot \mathbf{n})}{2(4 + f^2 + g^2)(4 + f_i^2 + g_i^2)},
\end{aligned} \tag{74}$$

$$\frac{\partial}{\partial f} (\mathbf{n}_s \cdot \mathbf{n}) = \frac{4(f_i - f) - 2f\sqrt{4 + f_i^2 + g_i^2}(\mathbf{n}_s \cdot \mathbf{n})}{(4 + f^2 + g^2)\sqrt{4 + f_i^2 + g_i^2}}, \tag{75}$$

$$\frac{\partial}{\partial g} (\mathbf{n}_s \cdot \mathbf{n}) = \frac{4(g_i - g) - 2g\sqrt{4 + f_i^2 + g_i^2}(\mathbf{n}_s \cdot \mathbf{n})}{(4 + f^2 + g^2)\sqrt{4 + f_i^2 + g_i^2}}, \tag{76}$$

$$\begin{aligned} \frac{\partial}{\partial f} \exp\left\{-c^2[\cos^{-1}(\mathbf{n}_s \cdot \mathbf{n})]^2\right\} &= \\ \frac{\partial}{\partial f} (\mathbf{n}_s \cdot \mathbf{n}) \frac{c^2 \cos^{-1}(\mathbf{n}_s \cdot \mathbf{n})}{\sqrt{1-(\mathbf{n}_s \cdot \mathbf{n})^2}} \exp\left\{-c^2[\cos^{-1}(\mathbf{n}_s \cdot \mathbf{n})]^2\right\}, \end{aligned} \quad (77)$$

$$\begin{aligned} \frac{\partial}{\partial g} \exp\left\{-c^2[\cos^{-1}(\mathbf{n}_s \cdot \mathbf{n})]^2\right\} &= \\ \frac{\partial}{\partial g} (\mathbf{n}_s \cdot \mathbf{n}) \frac{c^2 \cos^{-1}(\mathbf{n}_s \cdot \mathbf{n})}{\sqrt{1-(\mathbf{n}_s \cdot \mathbf{n})^2}} \exp\left\{-c^2[\cos^{-1}(\mathbf{n}_s \cdot \mathbf{n})]^2\right\}, \end{aligned} \quad (78)$$

$$\begin{aligned} R_1(f, g) = R_f(f, g) &\equiv \frac{\partial}{\partial f} R(f, g), \\ &= \rho_1 \frac{\partial}{\partial f} (\mathbf{n}_s \cdot \mathbf{n}) \frac{c^2 \cos^{-1}(\mathbf{n}_s \cdot \mathbf{n})}{\sqrt{1-(\mathbf{n}_s \cdot \mathbf{n})^2}} \\ &\exp\left\{-c^2[\cos^{-1}(\mathbf{n}_s \cdot \mathbf{n})]^2\right\} + \rho_2 \frac{\partial}{\partial f} (\mathbf{i} \cdot \mathbf{n}), \end{aligned} \quad (79)$$

$$\begin{aligned} R_2(f, g) = R_g(f, g) &\equiv \frac{\partial}{\partial g} R(f, g), \\ &= \rho_1 \frac{\partial}{\partial g} (\mathbf{n}_s \cdot \mathbf{n}) \frac{c^2 \cos^{-1}(\mathbf{n}_s \cdot \mathbf{n})}{\sqrt{1-(\mathbf{n}_s \cdot \mathbf{n})^2}} \\ &\exp\left\{-c^2[\cos^{-1}(\mathbf{n}_s \cdot \mathbf{n})]^2\right\} + \rho_2 \frac{\partial}{\partial g} (\mathbf{i} \cdot \mathbf{n}). \end{aligned} \quad (80)$$

Next, we consider the dependence of eigenvalue of  $Y(\mathbf{X}^*)$  on  $\rho_1$ . Because of the results of the preceding section, it suffices to only discuss

$$\mu = \frac{\gamma}{\left(\gamma + R_1^2 + R_2^2\right)}$$

which is smaller than 1. The derivatives of  $\mu$  with respect to  $\rho_1$  are given by

$$\frac{\partial \mu}{\partial \rho_1} = -2\gamma \frac{R_1 \frac{\partial R_1}{\partial \rho_1} + R_2 \frac{\partial R_2}{\partial \rho_1}}{\left(\gamma + R_1^2 + R_2^2\right)^2}. \quad (81)$$

For simplicity, we consider the near-Lambertian case ( $0 < \rho_1 \ll \rho_2$ ). In this case,

$$\theta_n^* \left( \frac{\theta_i \leq \theta_n^* \leq \theta_i}{2} \right)$$

is approximately represented as

$$\theta_n^* \approx \theta_i, \quad \theta_n^* - \frac{\theta_i}{2} \approx \theta_i - \frac{\theta_i}{2} = \frac{\theta_i}{2}. \quad (82)$$

When Eq. 16 is approximated by

$$a\rho_1 + \rho_2 \approx 1, \quad a \equiv \exp\left\{-c^2\left(\frac{\theta_i}{2}\right)^2\right\}. \quad (83)$$

Then, we have

$$\begin{aligned} \frac{\partial R_1}{\partial \rho_1} &= \frac{\partial}{\partial f} (\mathbf{n}_s \cdot \mathbf{n}) \frac{c^2 \cos^{-1}(\mathbf{n}_s \cdot \mathbf{n})}{\sqrt{1-(\mathbf{n}_s \cdot \mathbf{n})^2}} \exp \\ &\left\{-c^2[\cos^{-1}(\mathbf{n}_s \cdot \mathbf{n})]^2\right\} - a \frac{\partial}{\partial f} (\mathbf{i} \cdot \mathbf{n}), \end{aligned} \quad (84)$$

$$\begin{aligned} \frac{\partial R_2}{\partial \rho_1} &= \frac{\partial}{\partial g} (\mathbf{n}_s \cdot \mathbf{n}) \frac{c^2 \cos^{-1}(\mathbf{n}_s \cdot \mathbf{n})}{\sqrt{1-(\mathbf{n}_s \cdot \mathbf{n})^2}} \exp \\ &\left\{-c[\cos^{-1}(\mathbf{n}_s \cdot \mathbf{n})]^2\right\} - a \frac{\partial}{\partial g} (\mathbf{i} \cdot \mathbf{n}). \end{aligned} \quad (85)$$

Because eigenvalue

$$\mu = \frac{\gamma}{\gamma + R_1^2 + R_2^2} = \frac{\gamma}{\gamma + R_f^2 + R_g^2}$$

takes the maximum value when  $(f, g)$  satisfies the condition that  $R = R_{\max}$ , i.e.,  $R_f = R_g = 0$ ,  $\mu$  takes great value when  $R(f, g)$  nears  $R_{\max}$ . Therefore, we consider eigenvalue  $\mu$  at  $(f, g)$  such that  $R(f, g)$  nears  $R_{\max}$ . For the near-Lambertian case, when  $\mathbf{n} \approx \mathbf{i}$ , i.e.,  $f \approx f_i$  and  $g \approx g_i$ , we can obtain  $R \approx R_{\max}$ . Then, we only consider these  $(f, g)$  which near  $(f_i, g_i)$ . In this case, we have

$$\begin{aligned} \frac{\partial}{\partial f} (\mathbf{n}_s \cdot \mathbf{n}) &= \\ \frac{4(f_i - f) - 2f\sqrt{4 + f_i^2 + g_i^2}(\mathbf{n}_s \cdot \mathbf{n})}{(4 + f^2 + g^2)\sqrt{4 + f_i^2 + g_i^2}} &\approx \frac{-2f(\mathbf{n}_s \cdot \mathbf{n})}{4 + f^2 + g^2}, \end{aligned} \quad (86)$$

$$\begin{aligned} \frac{\partial}{\partial f} (\mathbf{i} \cdot \mathbf{n}) &= \\ 2 \frac{8f_i - (4 - f^2 - g^2)f - (4 + f_i^2 + g_i^2)f(\mathbf{i} \cdot \mathbf{n})}{(4 + f^2 + g^2)(4 + f_i^2 + g_i^2)} &\approx \\ 2 \frac{f[1 - (\mathbf{i} \cdot \mathbf{n})]}{4 + f^2 + g^2} \end{aligned} \quad (87)$$

Because  $\mathbf{n} \approx \mathbf{i}$ ,  $f \approx f_i$ , and  $g \approx g_i$ , we obtain  $(\mathbf{i} \cdot \mathbf{n}) \approx 1$ . Then, Eq. 87 becomes

$$\frac{\partial}{\partial f} (\mathbf{i} \cdot \mathbf{n}) \approx 0. \quad (88)$$

From Eqs. 79, 84, and 88, we have

$$R_1 \frac{\partial R_1}{\partial \rho_1} \approx \quad (89)$$

$$\rho_1 \left[ \frac{\partial (\mathbf{n}_s \cdot \mathbf{n})}{\partial f} \frac{c^2 \cos^{-1}(\mathbf{n}_s \cdot \mathbf{n})}{\sqrt{1-(\mathbf{n}_s \cdot \mathbf{n})^2}} \exp\left\{-c^2[\cos^{-1}(\mathbf{n}_s \cdot \mathbf{n})]^2\right\} \right]^2 \geq 0,$$

where  $R(f,g)$  nears  $R_{\max}$ . Similarly,

$$R_2 \frac{\partial R_2}{\partial \rho_1} \geq 0.$$

Then we have

$$\frac{\partial \mu}{\partial \rho_1} = -2\gamma \frac{R_1 \frac{\partial R_1}{\partial \rho_1} + R_2 \frac{\partial R_2}{\partial \rho_1}}{(\gamma + R_1^2 + R_2^2)^2} \leq 0, \quad (90)$$

From Eq. 90, when  $R(f,g)$  nears  $R_{\max}$ , the eigenvalue  $\mu$  decreases and the convergence speed of the iterative algorithm is faster as parameter  $\rho_1$  increases. But in the case far from Lambertian (non-Lambertian case), it seems that the precision of the inference of  $(f,g)$  deteriorates, because the brightness at the region near the occluding boundary becomes dark (only brightness at the region near specular point is bright).

### Numerical Experiment

To evaluate the proposed algorithm quantitatively, we show results of the numerical experiment. We assume that the direction of the light source is  $\theta_s = 10^\circ$ ,  $\phi_s = 0^\circ$ . We use an ellipsoid:

$$\frac{x^2}{30^2} + \frac{y^2}{25^2} + \frac{z^2}{25^2} = 1.$$

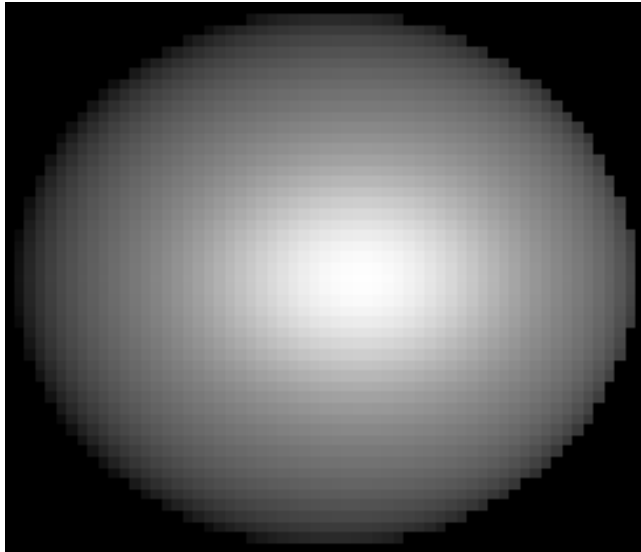


Figure 1. Image brightness ( $\rho_1 = 0.400$ ,  $\rho_2 = 0.602$ ).

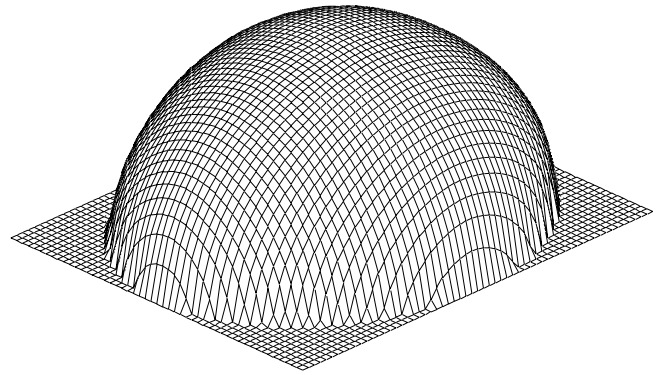


Figure 2. Reconstructed shape.

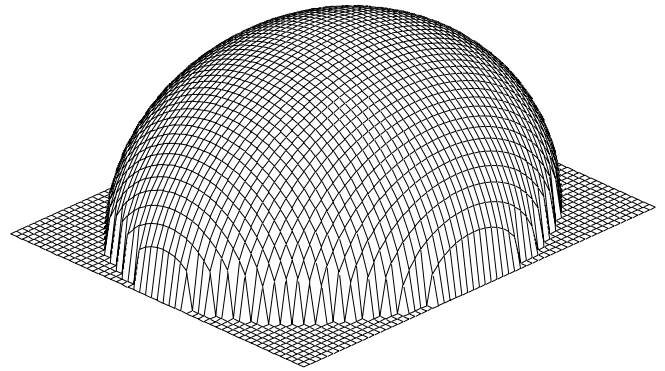


Figure 3. True shape.

Figure 1 shows the image brightness of this ellipsoid.

**Inference Precision of  $\rho_1$  and  $\rho_2$ .** Table I shows the results of the inference precision of parameters  $\rho_1$  and  $\rho_2$  for the case of Gaussian noise presence. In the table, “free” means the noise-free case and dB is defined as:

$$\text{dB} = 10 \log \text{SNR}$$

$$\text{SNR} = \hat{\sigma}^2 / \sigma^2, \quad \hat{\sigma}^2 = \frac{1}{N} \sum_i \sum_j (E_{ij} - \bar{E})^2,$$

where  $\sigma^2$  denotes the variance of Gaussian noise,  $N$  the number of image points corresponding to the object, and  $\bar{E}$  the mean value of  $E_{ij}$ .

**3-D Shape Inference.** Figure 2 illustrates the 3-D shape reconstructed by the proposed algorithm from the image brightness given by Fig. 1. The true 3-D shape is shown in Fig. 3. Figures 4 and 5 illustrate

TABLE I. Estimated Values of  $\rho_1$  and  $\rho_2$ .

true		estimated (free)		estimated (dB:40)		estimated (dB:30)		estimated (dB:20)	
$\rho_1$	$\rho_2$	$\rho_1$	$\rho_2$	$\rho_1$	$\rho_2$	$\rho_1$	$\rho_2$	$\rho_1$	$\rho_2$
0.0000	1.0000	0.0000	1.0000	0.0067	0.9933	0.0220	0.9789	0.0685	0.9332
0.1000	0.9020	0.1000	0.9020	0.1068	0.8952	0.1216	0.8806	0.1682	0.8342
0.2000	0.8023	0.2000	0.8023	0.2070	0.7954	0.2220	0.7803	0.2696	0.7327
0.3000	0.7023	0.3000	0.7023	0.3072	0.6951	0.3227	0.6795	0.3719	0.6303
0.4000	0.6021	0.4000	0.6021	0.4075	0.5946	0.4236	0.5784	0.4748	0.5271
0.5000	0.5018	0.5000	0.5018	0.5078	0.4939	0.5247	0.4770	0.5782	0.4233
0.6000	0.4015	0.6000	0.4015	0.6082	0.3932	0.6260	0.3754	0.6822	0.3190
0.7000	0.3011	0.7000	0.3011	0.7087	0.2924	0.7274	0.2736	0.7865	0.2143
0.8000	0.2008	0.8000	0.2008	0.8091	0.1916	0.8289	0.1718	0.8912	0.1092
0.9000	0.1004	0.9000	0.1004	0.9096	0.0907	0.9304	0.0698	0.9962	0.0038
1.0000	0.0000	1.0000	0.0000	1.0003	0.0008	1.0015	0.0020	1.0030	0.0040

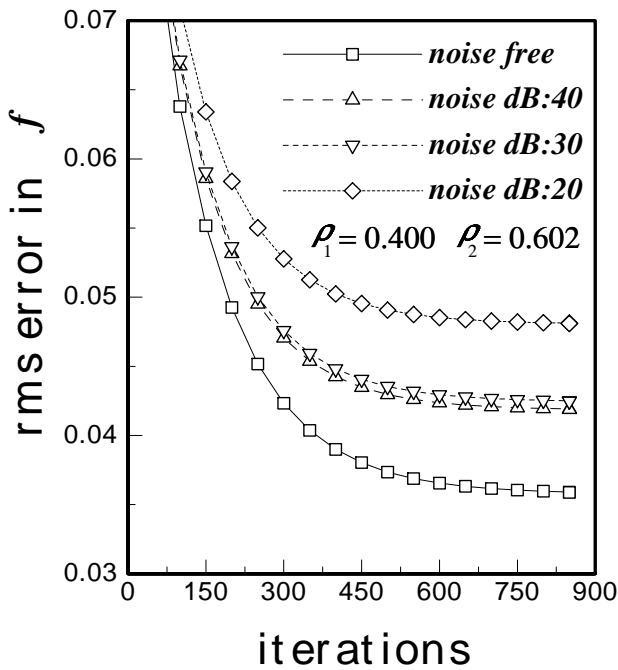


Figure 4. Rms error in  $f$  for case with noise presence.

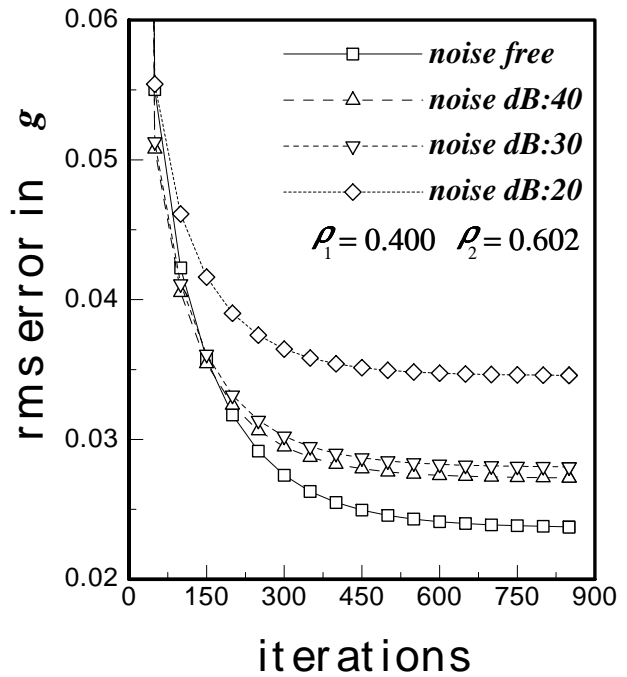


Figure 5. Rms error in  $g$  for case with noise presence.

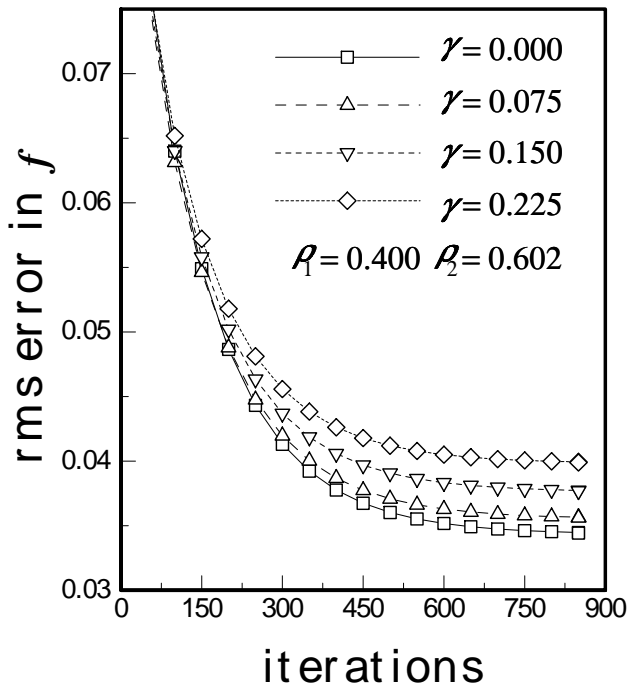


Figure 6. Rms error in  $f$  with  $\gamma$  as a parameter for case of fixed  $\rho_1$ .

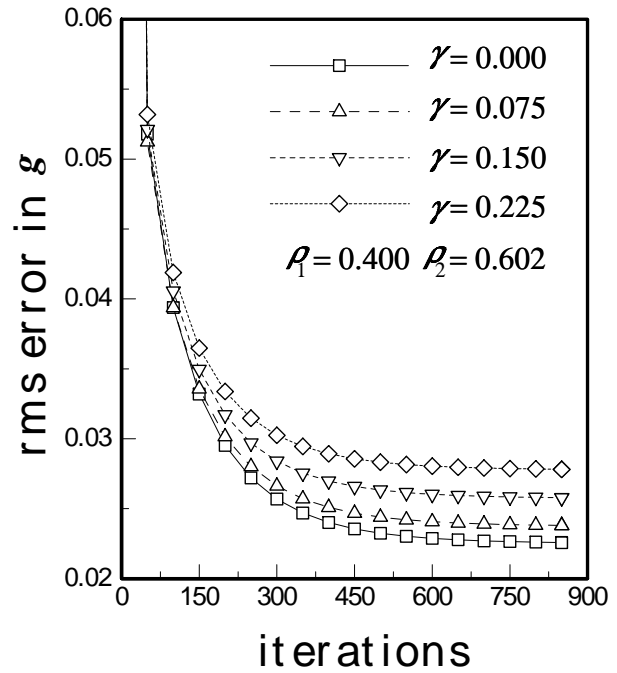


Figure 7. Rms error in  $g$  with  $\gamma$  as a parameter for case of fixed  $\rho_1$ .

rms errors in  $f$  and  $g$ , respectively, with noise level dB as a parameter.

**Relation between  $\gamma$  and Convergence Speed.** Figures 6 and 7 show that the convergence speed is dependent on  $\gamma$ . From Eq. 59 we can see that the convergence speed gets slow when  $\gamma$  increases.

**Relation between  $\rho_1$  and Convergence Speed.** Figures 8 and 9 illustrate that convergence speed is dependent on  $\rho_1$ .

As shown in section “**Dependence of Eigenvalue on  $\rho_1$ ,**” in the near-Lambertian case ( $\rho_1$  is small), the convergence of the iterative algorithm becomes fast as  $\rho_1$  increases. But in the non-Lambertian case ( $\rho_1$  is large), the brightness except for the specular point becomes dark. Then it is considered that the inference precision deteriorates because the brightness in the region neighboring the occluding boundary becomes dark.

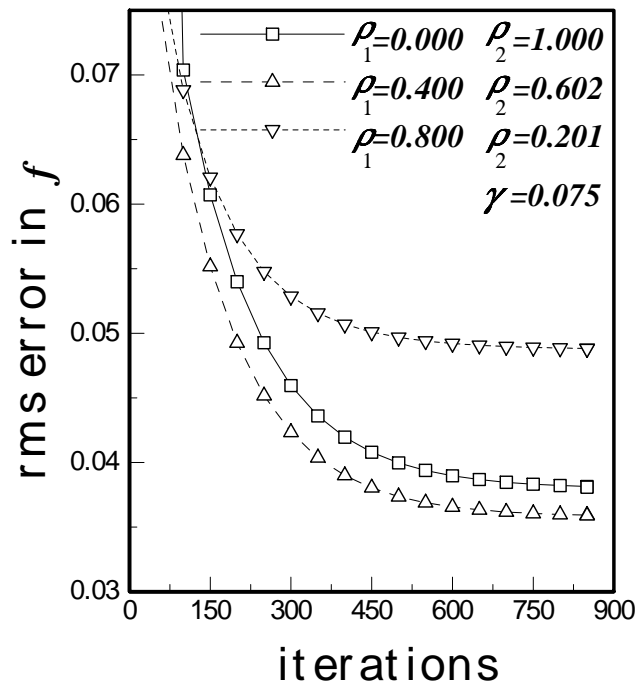


Figure 8. Rms error in  $f$  with  $\rho_1$  as a parameter for case of fixed  $\gamma$ .

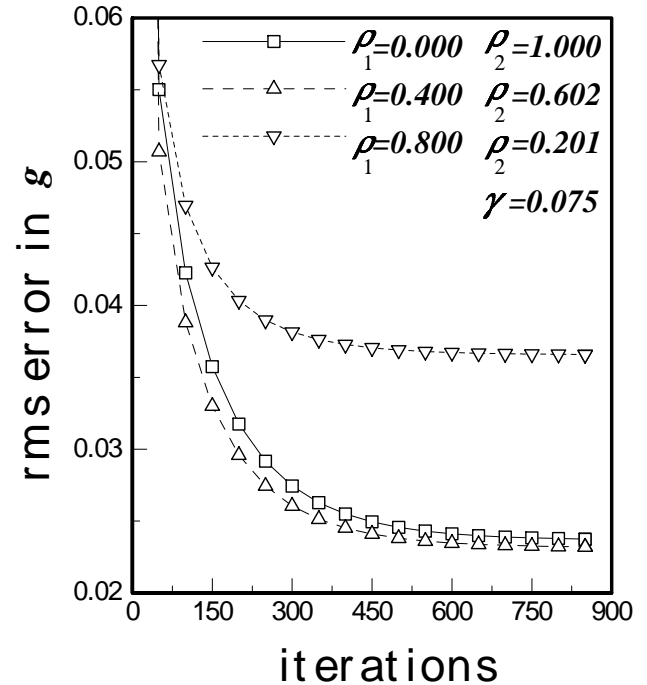


Figure 9. Rms error in  $g$  with  $\rho_1$  as a parameter for case of fixed  $\gamma$ .

### Conclusion

We have proposed a method for shape recovery from shading for non-Lambertian surfaces illuminated by only a single light source. In the method, parameters determining the reflectance map are identified by using occluding boundary information. Subsequently, the normal of the object surface is estimated, and 3-D shape is recovered. By theoretically considering the convergence of the proposed iterative algorithm, we have verified that the proposed algorithm converges, and that for the near-Lambertian case, the convergence speed becomes faster as  $\rho_1$  increases. ▲

### References

1. B. K. P. Horn, Understanding Image Intensities, *Art. Int.*, **8**, 201–231 (1977).
2. K. Ikeuchi and B. K. P. Horn, Numerical shape from shading and occluding boundaries, *Art. Int.*, **17**, 141–184 (1981).
3. R. Onn and A. Bruckstein, integrability disambiguates surface recovery in two-image photometric stereo, *Int. J. Comp. Vis.*, **5**, 105–113 (1990).
4. K. Ikeuchi, Determining the surface orientations of specular surfaces by using the photometric stereo method, *IEEE Trans. PAMI-3*, 661–669 (1981).
5. E. N. Coleman and R. Jain, Obtaining 3 dimensional shape of textured and specular surfaces using four-source photometry, *CVGIP* **18**, 309–328 (1982).
6. H. D. Tagare and R. J. P. deFigueiredo, A theory of photometric stereo for a class of diffuse non-lambertian surface, *IEEE Trans. PAMI-13*, 133–152 (1991).
7. H. D. Tagare and R. J. P. deFigueiredo, Simultaneous estimation of shape and reflectance map from photometric stereo, *CVGIP: Image Unde.* **55**, 275–286 (1992).
8. F. Solomon and K. Ikenchi, Extracting the shape and roughness of specular lobe objects using four light photometric stereo, *IEEE Trans. PAMI-18*, 449–454 (1996).
9. K. E. Torrance and E. M. Sparrow, Theory for off-specular reflection from roughened surfaces, *J. Opt. Soc. Am.* **56**, 1105–1114 (1967).
10. J. M. Ortega and W. C. Rheinboldt, *Iterative Solution of Nonlinear Equations in Several Variables*, Academic Press, New York, p. 281, 1970.